



# The first complete inventory of the local glaciers and ice caps on Greenland

P. Rastner<sup>1</sup>, T. Bolch<sup>1,2</sup>, N. Mölg<sup>1</sup>, H. Machguth<sup>1,3</sup>, R. Le Bris<sup>1</sup>, and F. Paul<sup>1</sup>

<sup>1</sup>Department of Geography, University of Zurich, Zurich, Switzerland

<sup>2</sup>Institute for Cartography, Technische Universität Dresden, Dresden, Germany

<sup>3</sup>Marine Geology and Glaciology, Geological Survey of Denmark and Greenland – GEUS, København, Denmark

Correspondence to: P. Rastner (philipp.rastner@geo.uzh.ch)

Received: 11 June 2012 – Published in The Cryosphere Discuss.: 16 July 2012

Revised: 8 November 2012 – Accepted: 13 November 2012 – Published: 10 December 2012

**Abstract.** Glacier inventories provide essential baseline information for the determination of water resources, glacier-specific changes in area and volume, climate change impacts as well as past, potential and future contribution of glaciers to sea-level rise. Although Greenland is heavily glacierised and thus highly relevant for all of the above points, a complete inventory of its glaciers was not available so far. Here we present the results and details of a new and complete inventory that has been compiled from more than 70 Landsat scenes (mostly acquired between 1999 and 2002) using semi-automated glacier mapping techniques. A digital elevation model (DEM) was used to derive drainage divides from watershed analysis and topographic attributes for each glacier entity. To serve the needs of different user communities, we assigned to each glacier one of three connectivity levels with the ice sheet (CL0, CL1, CL2; i.e. no, weak, and strong connection) to clearly, but still flexibly, distinguish the local glaciers and ice caps (GIC) from the ice sheet and its outlet glaciers. In total, we mapped  $\sim 20\,300$  glaciers larger than  $0.05\text{ km}^2$  (of which  $\sim 900$  are marine terminating), covering an area of  $130\,076 \pm 4032\text{ km}^2$ , or  $89\,720 \pm 2781\text{ km}^2$  without the CL2 GIC. The latter value is about 50 % higher than the mean value of more recent previous estimates. Glaciers smaller than  $0.5\text{ km}^2$  contribute only 1.5 % to the total area but more than 50 % (11 000) to the total number. In contrast, the 25 largest GIC ( $> 500\text{ km}^2$ ) contribute 28 % to the total area, but only 0.1 % to the total number. The mean elevation of the GIC is 1700 m in the eastern sector and around 1000 m otherwise. The median elevation increases with distance from the coast, but has only a weak dependence on mean glacier aspect.

## 1 Introduction

Glaciers and ice caps (GIC in the following) are key indicators of climate change (e.g. Lemke et al., 2007), important water resources and their melt water could potentially make a substantial contribution to sea-level rise during this century (e.g. Meier et al., 2007; Hock et al., 2009; Radić and Hock, 2010). Related assessments require accurate knowledge about their location and extent as available in glacier inventories. The periphery of the Greenland Ice Sheet is one of the regions with a potentially large contribution to sea-level rise, but inventory information is incomplete and digital outlines are missing (Kargel et al., 2012). Moreover, the situation in Greenland is special due to the highly complex boundary between the ice sheet and its outlet glaciers and the local GIC (Paul, 2011). To overcome this problem and to provide a sound database for global-scale modelling applications (e.g. Huss and Farinotti, 2012; Radić and Hock, 2010), a complete dataset (vector outlines) of all GIC on Greenland is an urgent demand.

So far, only parts of Greenland's GIC have been inventoried in detail: the inventory of west Greenland (Weidick et al., 1992), the Geikie Plateau and Scoresby Sund region inventory (Jiskoot et al., 2003, 2012) and the inventory of Disko Island and the Nuussuaq – Svartenhuk peninsulas (Citterio et al., 2009). Only two datasets (Geikie plateau and South Kronprins Christian Land) are downloadable from the Global Land Ice Measurements from Space (GLIMS, www.glims.org) database. The two currently available Greenland-wide vector datasets of the total ice-covered area are the GIMP (Greenland Ice sheet Mapping Project)

dataset (available at: <http://bprc.osu.edu/GDG/icemask.php>) (Howat and Negrete, 2012) and the rather coarse outlines from the Digital Chart of the World (DCW, Danko, 1992). However, both datasets do not separate the local GIC from the ice sheet or from each other, i.e. they only show contiguous ice masses (or glacier complexes) without drainage divides. A similarly comprehensive dataset with vector outlines of all GIC and the ice sheet is held by GEUS based on map data from the 1980s, but not (yet) available for scientific research (Citterio and Ahlstrøm, 2012). All of the above datasets vary in their degree of generalisation, temporal frame, and consideration of details (e.g. debris cover or ice shelves).

Due to the lack of complete inventory data (the DCW was never used for that purpose) the total area covered by local GIC on Greenland has been assessed by a range of (not always fully documented) techniques. The more recently reported values range from about 49 000 km<sup>2</sup> (Ohmura, 2009; Weidick and Morris, 1998) up to 76 200 km<sup>2</sup> (Dowdeswell and Hambrey, 2002; Weidick and Morris, 1998). Despite the large area covered (approximately 7 % of all GIC worldwide, cf. Hock et al., 2009), the calculation of the sea-level rise contribution of Greenland's GIC has received only limited attention. The absence of a consistent and complete inventory required the application of rough extrapolation schemes (Radić and Hock, 2010), their complete exclusion (Raper and Braithwaite, 2006), or a separate treatment (Lemke et al., 2007).

For the above reasons we have compiled the first glacier inventory of all GIC in Greenland by applying semi-automated glacier-mapping techniques (e.g. Paul and Kääb, 2005) to more than 70 Landsat scenes. In combination with a digital elevation model (DEM) drainage divides were derived following Bolch et al. (2010) and digitally intersected with the glacier outlines to obtain individual glaciers and to calculate topographic parameters for each entity from the DEM following Paul et al. (2009). A rather challenging issue in this regard was to define a consistent strategy for separating the GIC from the ice sheet, as the local GIC occur not just in coastal regions away from the ice sheet, but also on mountain ridges within and adjacent to the ice sheet (Weidick and Morris, 1998). Considering the varying requirements of the different scientific communities (e.g. sea-level change or hydrological and glaciological modelling), we assigned three connectivity levels (CL) to all GIC describing the strength of connection (no, weak, strong) to the ice sheet. This distinction is required, for instance, to avoid double counting of their contribution to sea-level rise, as the normally used ice masks for the Greenland Ice Sheet also include (at least partly) local GIC (Paul, 2011).

The main purposes of the inventory presented here are thus to close the knowledge gap about the local GIC on Greenland and to provide a sound base for proper change assessment (Kargel et al., 2012). While the full dataset will be made available through the GLIMS database (Bishop et al., 2004;

Raup et al., 2007), the outlines along with their connectivity levels have already been made available within the Randolph Glacier Inventory (RGI) documented by Arendt et al. (2012).

## 2 Study region and datasets

### 2.1 Study region

Our study region is the whole of Greenland (Fig. 1), extending from 60° to 84° N (2650 km) and from 11° to 74° W (1200 km). More than 80 % of Greenland is covered by ice ranging from sea level to 3200 m a.s.l. at the central dome of the ice sheet and to almost 3700 m a.s.l. on Greenland's highest mountain (Gunnbjørn Fjeld). To provide a more regionalised assessment of the GIC characteristics, we divided Greenland into seven glaciological subregions (Fig. 1) following the suggestion of Weidick (1995), but combining the southern part in two sectors. All place names used in this study are based on Weidick (1995) with missing names being added from Rignot and Mouginot (2012).

Greenland's climate is polar to sub-polar. The island acts climatologically as a centre of cooling, and hydrologically as a large store of freshwater. Temperatures in Greenland have been monitored since the 1870s, showing a warming trend since the 1980s that increased during the 1990s predominantly on the western coast (Cappelen et al., 2007). The year 2010 was the warmest year across Greenland (except for the northeast) since the start of meteorological observations (Box et al., 2006). The present-day accumulation pattern in Greenland is roughly captured by measurements (Bales et al., 2009; Burgess et al., 2010) and regional climate modelling (Box et al., 2006; Ettema et al., 2009; Fettweis et al., 2008), with large uncertainties remaining in regions where measurements are sparse (Helsen et al., 2012). According to Ohmura and Reeh (1991), the highest annual precipitation amounts occur south of 65° N on the western side (400–1000 mm a<sup>-1</sup>) and south of 70° on the eastern side (400–2500 mm a<sup>-1</sup>) of Greenland. The lowest amounts are found in the northeastern interior (100 mm a<sup>-1</sup>) and locally around Søndre Strømfjord on the western coast and Narssarssuaq in southern Greenland.

A large variety of glacier types from ice caps with numerous outlet glaciers, to valley and mountain glaciers of all shapes and cirques are found in Greenland. Due to the large north–south extent, different thermal regimes can be expected for the glaciers. Whereas in the north most GIC are cold, they are polythermal in the central part and in the south also temperate GIC are found (Bull, 1963; Hammer, 2001). Several glaciers on Greenland were identified as being of surge type; for instance in the Stauning Alper and Geikie Plateau region (Jiskoot et al., 2003, 2012; Weidick, 1988) but also in the Disko/Nuussuaq region (Yde and Knudsen, 2005).

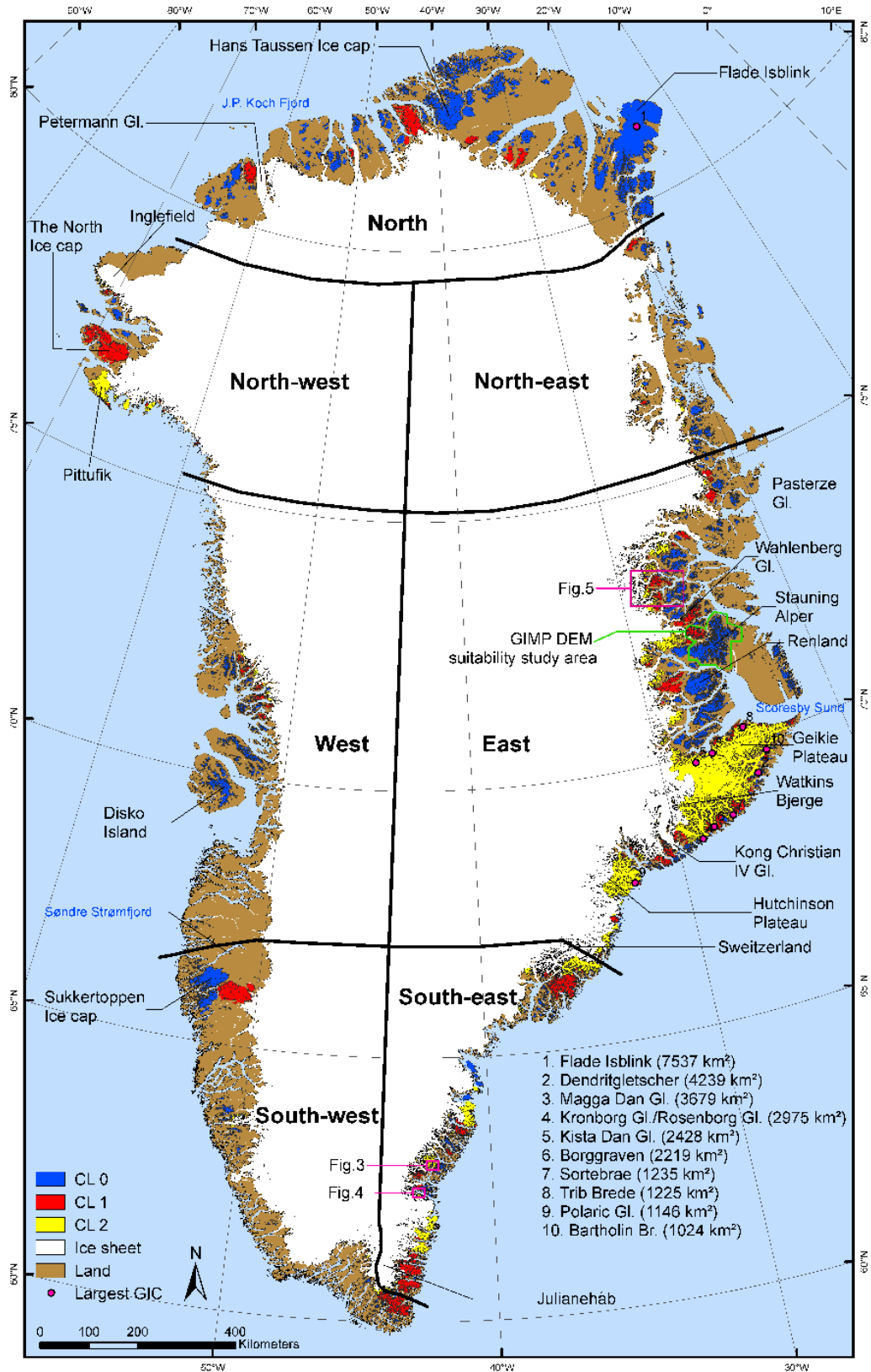


**Fig. 1.** Map of Greenland showing all local GIC (colour coded) and place names mentioned in the text. The green box indicates the area selected for the investigation of DEMs and the magenta ones the location of Figs. 3, 4 and 5.

## 2.2 Datasets

We selected 73 of the most suitable (with minimum seasonal snow, and largely cloud free) Landsat scenes available from the [glovis.usgs.gov](http://glovis.usgs.gov) archive, focussing on Landsat 7 ETM+ scenes (1999–2002) dating from before the failure of the scan line corrector (SLC) in 2003 (Table S1 and Fig. S1). Seasonal snow was a severe problem in the north-eastern part of Greenland and we mosaicked several SLC-off scenes from the years 2003 to 2008 with much better snow conditions to get an appropriate coverage. We also used some Landsat TM scenes from the period 1994 to 2008 to fill remaining data gaps. It has to be noted that during this period some glaciers have shown considerable changes in extent (e.g. Yde and Knudsen, 2005). The acquisition date of each scene processed is documented in the attribute table of each glacier polygon, so that a reference for change assessment is available.

To address the missing coverage with Landsat data north of 80° N, we used the outlines of the GIMP ice cover map that is available online at <http://bprc.osu.edu/GDG/icemask.php> (Howat and Negrete, 2012) as a baseline dataset. The GIMP ice cover map mostly excludes debris-covered glacier parts and glaciers smaller than 0.05 km<sup>2</sup>. In the northernmost region, ice shelves were included as the purpose of the GIMP dataset is to consider all ice-covered areas. We improved the GIMP outlines by visual interpretation of a MODIS 250 m image of the same region. This was important as ice shelves and some wrongly classified ice-covered lakes adjacent to outlet glaciers of the Hans Tausen Ice Cap (cf. Hammer, 2001) had to be removed for our purpose.

For our inventory, we decided to stick to the DEM of the Greenland Ice sheet Mapping Project (GIMP, Howat et al., 2012) with the supplement tile “GI-north” from the website [www.viewfinderpanoramas.org](http://www.viewfinderpanoramas.org) (VFP) in the very far north that was not covered by the GIMP DEM. The GIMP DEM has a resolution of 90 m and a reported vertical accuracy of 10 m (Howat et al., 2012). It was merged from several datasets acquired between the years 2000 and 2009. As high-resolution photogrammetric DEM extraction only provides accurate results in regions with good optical contrast and is therefore less accurate above the snow line, coarser resolution DEM data (500 m Advanced Very High Resolution Radiometer, AVHRR) was merged with the GIMP DEM (Howat et al., 2012). The VFP DEMs were mainly created from 1 : 250 000 and 1 : 500 000 scale topographic maps with locally variable quality (Ferranti, 2012). Additionally, the ASTER GDEM II (<http://reverb.echo.nasa.gov/reverb/>) was used to assess the suitability of the GIMP DEM for extracting topographic parameters in the Stauning Alper region.

## 3 Methods

The data processing workflow can roughly be subdivided into three steps (Fig. 2): (a) glacier mapping and editing, (b) creation of drainage divides to separate the local GIC from the ice sheet and from each other, and (c) intersection of the edited glacier outlines with the drainage divides, and a subsequent calculation of glacier-specific statistics using again the DEM. These three steps are described in the following in more detail.

### 3.1 Glacier mapping

For the glacier mapping we applied the well-established semi-automated band ratio method (e.g. Paul and Andreassen, 2009) using the raw digital numbers of Landsat ETM+ bands 3 (red) and 5 (shortwave infrared/SWIR). An optimal threshold for the ratio image was chosen interactively for each scene with pixels being classified as ice when the band 3/band 5 ratio exceeded 1.6 or slightly higher values (scene dependent). For several scenes an additional threshold in band 1 (blue) was applied to improve the mapping in shadow regions where path radiance otherwise introduces misclassification (cf. Paul and Kääb, 2005). In the next step, a median filter (3 × 3 kernel) was applied to reduce noise and the classified raster image was converted into a vector format (shapefile). Clean ice was accurately mapped by the algorithm and did not require manual correction for scenes with good snow conditions. However, the corrections for clouds, shadow, debris cover, seasonal snow and icebergs were time consuming, and took approximately 80 % of the total processing time (see examples in Figs. 3 and 4). Similar to the experience in other regions (e.g. Paul and Andreassen, 2009; Bolch et al., 2010), one of the most challenging questions was related to the correct consideration of extended snow fields that showed no ice but might be perennial rather than seasonal. As a general rule, we included all polygons showing ice and excluded most of the “snow only” polygons, in particular at low elevations. Moreover, most snow patches were removed by applying a size threshold of < 0.05 km<sup>2</sup>. The correct identification of frozen lakes was in some regions also difficult, a well-known problem when working in Arctic regions (e.g. Paul and Kääb, 2005; Racoviteanu et al., 2009). In this study we have additionally used DEM information (hillshades) and multi-temporal satellite images to improve their identification. The mapping and the manual corrections were always performed in the local UTM system of the respective scene (all scenes together spanning UTM zones 18–28). After that, the resulting outlines were mosaicked and reprojected with an area-preserving projection (Greenland Lambert Azimuthal Equal Area projection with D WGS 1984 datum), as the UTM projection is not area preserving.

The accuracy of the glacier outlines is difficult to assess as appropriate reference data are required but were not available for this region. However, a recent round robin experiment has



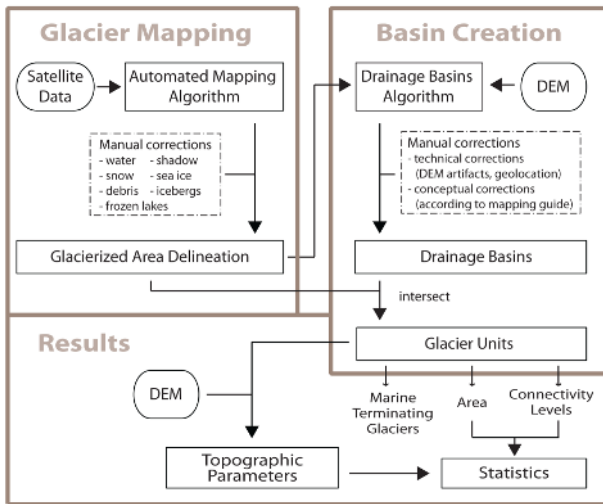


**Fig. 2.** Schematic flow chart illustrating the connection of the individual processing steps.

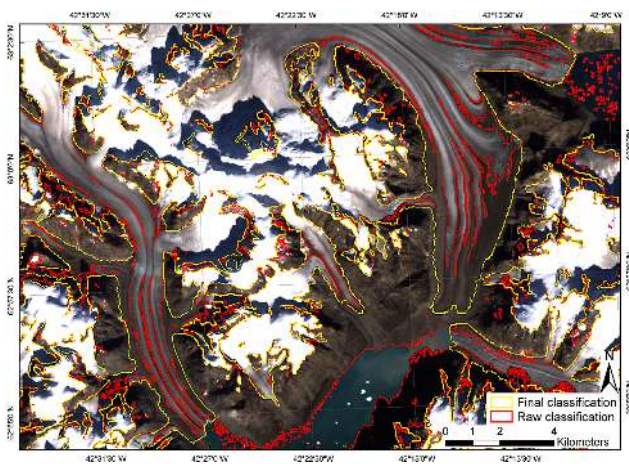


**Fig. 3.** Close-up of the raw classification (red) and the result after manual correction (yellow) (Landsat ETM+, 233 016, 10 September 2001).

analysed accuracy issues in more detail (Paul et al., 2012) comparing outlines derived automatically and from multiple manual digitisation of the same set of glaciers by the same and different analysts. The study concluded that the two methods (manual and automated) have about the same precision for clean ice (standard deviations between 2 and 5 %) and that results for debris-covered ice were strongly variable, with area differences exceeding 30 %. For clean ice, the locations of manually-digitized outlines were found to vary by about 1 TM pixel or 30 m (Paul et al., 2012). We thus determined the precision of the outlines derived here by applying a +15 m buffer around all glacier complexes (cf. Bolch et al., 2010). Adding this uncertainty gives a 3.1 % larger total area,

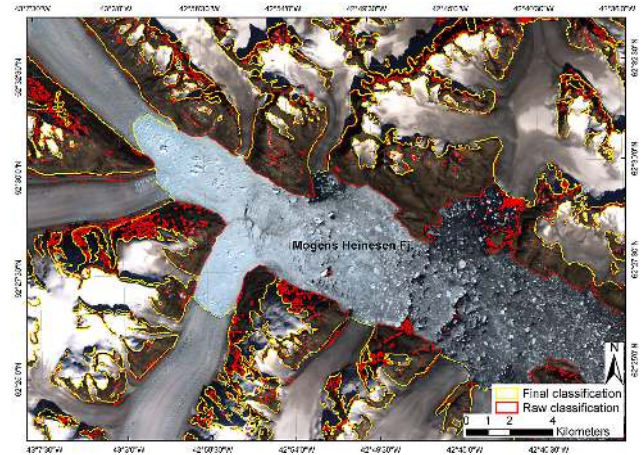


**Fig. 4.** Sea ice in front of marine terminating glaciers is mapped correctly with the band ratio method and has to be manually removed afterwards (Landsat ETM+, 233 016, 10 September 2001).

which is in the following used as a measure of uncertainty for the derived area values.

### 3.2 Drainage divides and assignment of connectivity levels

We derived drainage divides to separate the glacier complexes into individual glaciers in a two-step approach: First, drainage divides were automatically calculated by the GIS using watershed analysis following a modified version of an approach developed by Bolch et al. (2010), and in a second step they were manually adjusted using a colour-coded flow direction grid in the background.

The separation of local GIC was actually rather challenging, as outlet glaciers from otherwise disconnected ice caps can join outlets from the ice sheet (and thus contribute to their flow), or glaciers that are connected to the ice sheet in the accumulation region can have completely separated ablation regions. To serve the varying requirements of different communities (e.g. hydrological and glaciological modelling), we defined three connectivity levels (CL) of the GIC with the ice sheet:

- CL0: no connection;
- CL1: weak connection (clearly separable by drainage divides in the accumulation region, not connected or only in contact in the ablation region);
- CL2: strong connection (difficult to separate in the accumulation region and/or confluent flow in the ablation region).

To assign the connectivity level automatically in the GIS, we also applied a “topological heritage” rule. Glacier entities connected to other entities that have been assigned CL1 will adopt the same class. This is also the case for entities

connected to CL2 entities. CL0 entities (either individual or within a group of connected entities) have no connection to the ice sheet or any of the CL1 or CL2 GIC. A colour-coded illustration of the assigned connectivity levels is depicted in Fig. 5.

Indeed, the topological heritage rule could only be applied after the glacier complexes were separated into distinct entities. And here the next set of challenges started: as pointed out by Racoviteanu et al. (2009), separating an ice cap into entities is difficult from a methodological point of view and it can be discussed if an ice cap should be separated into entities at all (glaciological vs. hydrological application). A further issue is that a watershed algorithm can find a very large number of divides for an ice cap with a near symmetric shape that do not make sense even from a hydrological point of view. This changes when an ice cap has prominent outlet glaciers and at least some topographic variability such as the Jostedalbreen ice cap in Norway (Paul et al., 2011). The further set of rules to separate the glacier-complexes consistently is:

- GIC rule I: divide an ice cap only when it has prominent outlet glaciers and at least some topographic variability in the accumulation area.
- GIC rule II: if one outlet glacier is separated, the entire ice cap has to be divided into entities.
- GIC rule III: for ice caps and glacierised mountain flanks, the fewest number of glaciers should be created, only considering the most prominent topographic divides.

We are aware that rule III is a very subjective one. As an example, we show in Fig. 6 two larger ice caps. Only one of the ice caps is subdivided, as the other one has no topographic variability and no prominent outlet glacier. The correction of the raw drainage divides provided by the automated flowshed algorithm according to the rules above was a tedious and time-consuming work for all local GIC on Greenland. To support interpretation, we additionally used a hillshade and contour lines from the DEM, as well as contrast enhanced versions of the respective Landsat scenes.

### 3.3 Topographic parameters and DEM accuracy

Finally, the glacier outlines were digitally intersected with the drainage divides to obtain the glacier entities (cf. Bolch et al., 2010; Paul et al., 2002). This dataset is then digitally combined with the DEM and products thereof to derive a set of topographic parameters (area, minimum, maximum, mean and median elevation, mean slope and aspect) from the zonal statistics function in the GIS (calculates statistics on values of a raster dataset within the zones of another dataset) following Paul et al. (2009). As the smallest glacier in the sample (0.05 km<sup>2</sup>) covers only about six cells in the GIMP DEM, the quality of the derived parameters is reduced for

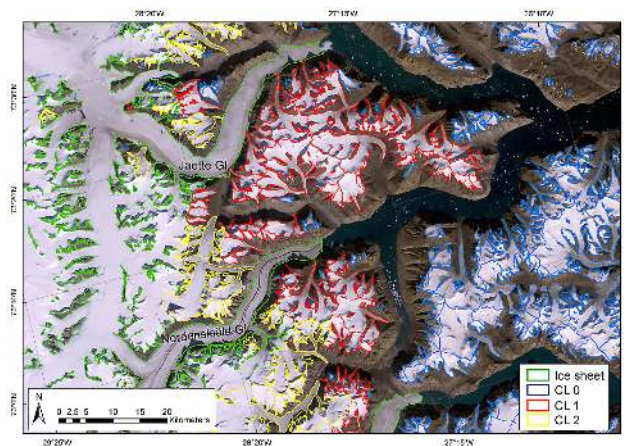


**Fig. 5.** Close-up of the assigned connectivity levels (colour-coded). Glaciers in contact with the ice sheet get their connectivity level first. Afterwards connected neighbouring polygons adopt the connectivity level, and finally disconnected glaciers are assigned to CL0 (Landsat ETM+, 232 008, 18 August 2001).

such small glaciers. We have thus calculated for a subset of 620 glaciers in the Stauning Alper region (see Fig. 1 for location) the minimum, maximum, mean and median elevation with the GIMP DEM and the ASTER GDEM II. A visual comparison of the hillshades of both DEMs highlights the much more uneven surface (with many artefacts) in the GDEM (Fig. 7). Although the standard deviation of the differences between individual glaciers are rather high (minimum: 636 m, maximum: 609 m, mean: 546 m, and median: 391 m) we found that the differences of these parameters between the two DEMs are rather small in the mean (minimum: 67 m, maximum: –46 m, mean: 1 m, and median: 3 m). On that basis we deemed the GIMP DEM acceptable also for small glaciers.

## 4 Results

In Fig. 1 we show an overview of all local GIC and their connectivity level. Three large regions, the Pittufik in the north-west, the entire Geikie Plateau with some glaciers of the Watkins Bjerger area and the Hutchinson Plateau in the east, and some smaller regions have CL2 connectivity according to our rules. In the southern sectors, we defined the peninsula in the south-east of Sweitzerland as CL1, together with three further peninsulas in the far south-east and the Sukkertoppen Ice Cap. In the northern sectors, we classified the North Ice Cap, the ice cap touching Petermann Glacier at the western side, and the ice cap south of J. P. Koch Fjord as CL1. The most prominent examples for the CL1 class in the eastern sector are the two ice caps located at the north and south of Pasterze Glacier, the two ice caps south of Wahlenberg Glacier and the ice cap in the east of Renland (see Fig. 1 for location).



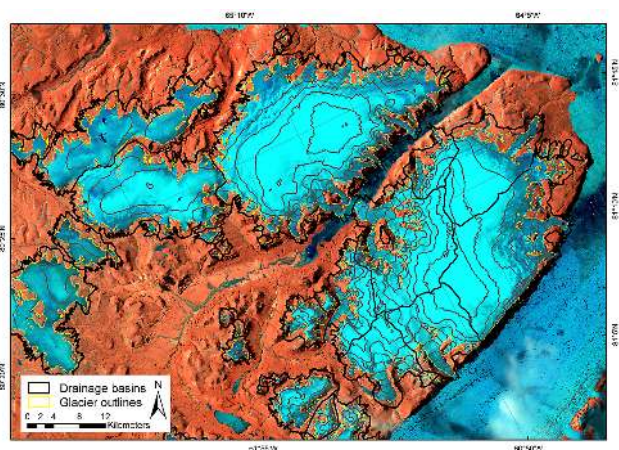


**Fig. 6.** Separation of ice caps into glacier entities and from each other. Though the large ice cap in the upper centre has several distinct outlet glaciers, it is not separated, as topographic structure is missing in the accumulation area (Landsat ETM+, 045 001, 30 June 2000).

Considering only entities larger than  $0.05 \text{ km}^2$ , all CL0 and CL1 GIC have a total area of  $89\,720 \pm 2781 \text{ km}^2$ . CL2 glaciers add  $40\,355 \pm 1251 \text{ km}^2$  for a total of  $130\,076 \pm 4032 \text{ km}^2$  and  $\sim 20\,300$  GIC overall. The ice sheet itself has an area of  $\sim 1\,678\,500 \pm 52\,033 \text{ km}^2$  according to our dataset and the entire ice covered area in Greenland is thus  $\sim 1.8$  million  $\text{km}^2$ . Hence, the area covered by the local GIC is  $\sim 7.2 \%$  of the total ice-covered area (Table 1). From the entire sample (including CL2), 904 (4.5 %) GIC are identified as marine terminating with an area of  $64\,975 \pm 2014 \text{ km}^2$  (Table S2). They are mostly found in the south-east and east of Greenland (Fig. S2). The area covered by marine terminating glaciers in the Geikie Plateau is  $24\,494 \text{ km}^2$  in our study and thus considerably lower than in the study by Jiskoot et al. (2012) who found  $37\,432 \text{ km}^2$ . This is because in the latter study Kong Christian IV Glacier is included, while we have excluded this large glacier due to a very long and uncertain divide on shallow ice ridges. Subtracting the area of Kong Christian IV Glacier ( $11\,079 \text{ km}^2$ ) from the area determined by Jiskoot et al. (2012) yields an area of  $26\,352 \text{ km}^2$  which is quite close to our result ( $\pm 750 \text{ km}^2$ ), considering the error bounds in both inventories.

Plotting the area covered and number of glaciers per size class separately for the seven sectors, all glaciers and the marine terminating glaciers only, reveals interesting differences (Fig. 8). In six subregions and Greenland as a whole the size classes  $0.1\text{--}0.5$  and  $1.0\text{--}5.0 \text{ km}^2$  have the highest relative contributions by number (about 35 and 20 %, respectively), but together they account for only a small part (10 %) of the total area. In contrast, glaciers larger than  $10 \text{ km}^2$  contribute only 8 % to the number but nearly 84 % to the total area in these regions. This is rather different for the marine terminat-

**Table 1.** Area covered and number of GIC for each connectivity level and the ice sheet.

	Area [ $\text{km}^2$ ]	Number
CL0	$65\,474 \pm 2029$	17 508
CL1	$24\,246 \pm 751$	1815
CL2	$40\,355 \pm 1251$	957
Total GIC	$130\,076 \pm 4032$	20 280
Ice sheet	$1\,678\,500 \pm 52\,033$	1
Total ice cover Greenland	$1\,808\,575 \pm 56\,065$	20 281

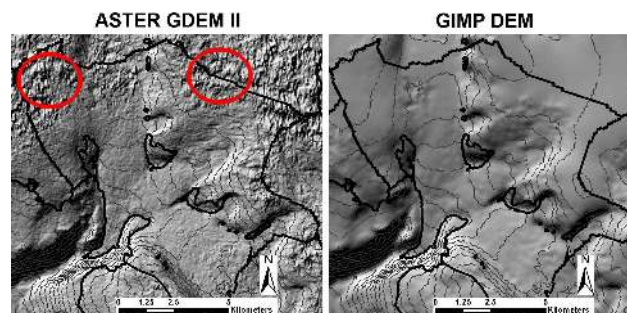


**Fig. 7.** Comparison of hillshades derived from the GIMP DEM and the ASTER GDEM II for a small subregion in the test area. Red circles indicate artefacts in the ASTER GDEM II that likely result from poor contrast in snow-covered regions.

ing glaciers where glaciers  $> 5 \text{ km}^2$  contribute 64.3 % to the total number and 98 % to the total area; i.e. their mean size is much larger ( $71.8 \text{ km}^2$ ) compared to the other regions (Table S3). In absolute terms, the largest glaciers are found in the east and northern sectors (Fig. 8; Table S3) followed by the southern and west sectors. The second largest of the size classes ( $100\text{--}500 \text{ km}^2$ ) is dominant in the north-west where large ice caps are present. Small glaciers are mostly found in the southern and western sectors.

The size distribution by aspect sector for CL0 and CL1 glaciers is listed in Table S4 (absolute values) and illustrated in Fig. 9 (relative values). The distribution is rather uniform for the two south as well as the east and west sectors (Fig. 9a), but concentrated towards SW for the sector north, towards N and S in the north-west sector and again rather uniform for the north-east sector (Fig. 9b). The SW exposition is also dominant for the whole of Greenland.

The area-elevation distributions for each sector and all of Greenland are depicted in Fig. 10 for all classes, and for the sector east and entire Greenland also with CL0 and CL1 separately. The largest ice-covered areas can be found in the north and east sectors, with remarkably different maxima around  $1000 \text{ m a.s.l.}$  and  $1700 \text{ m a.s.l.}$ , respectively. The lower maximum in the northern sector can be ascribed to the predominance of ice caps, and likely also to the lower mean annual air temperature (MAAT) in this region. The special topography of the numerous ice

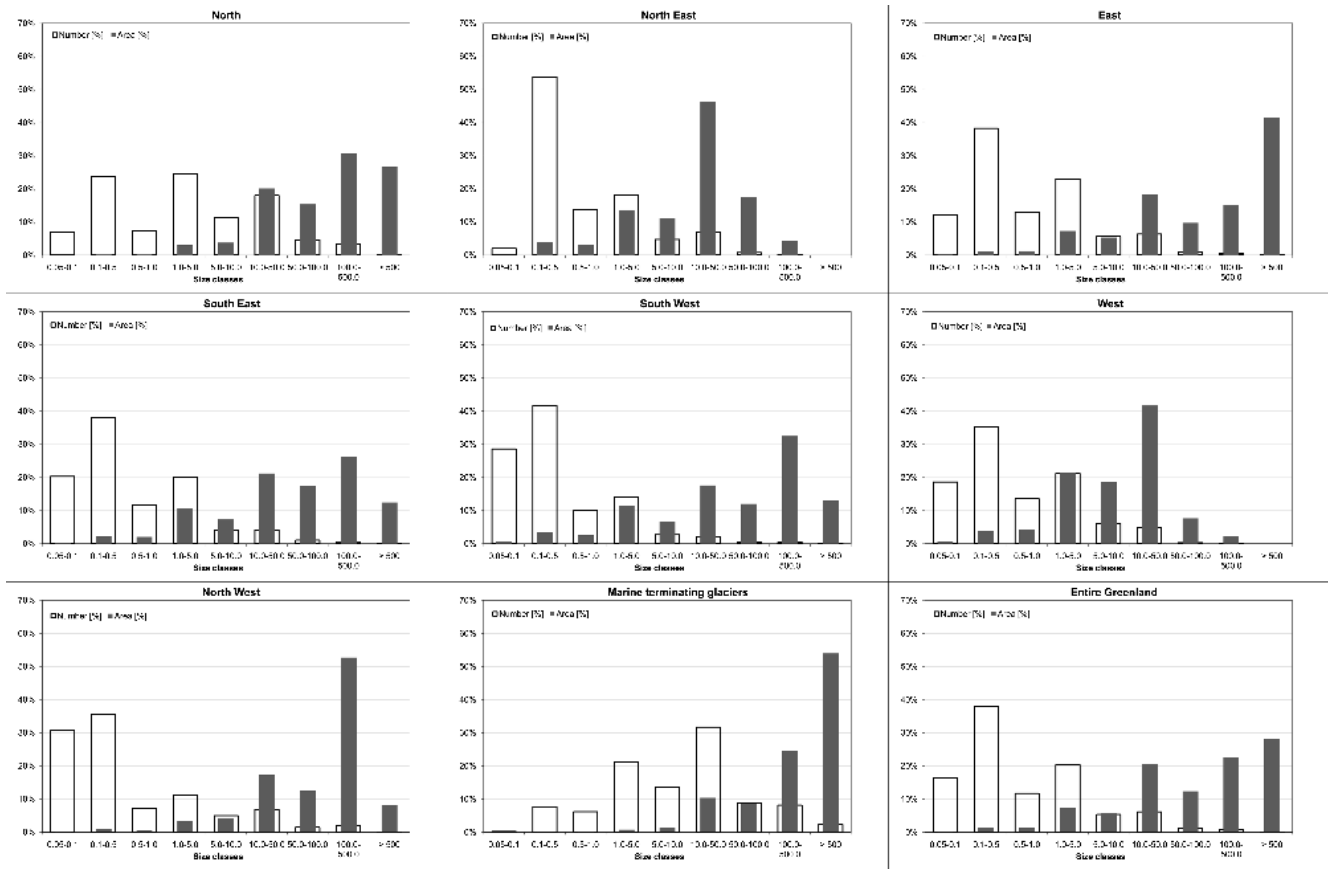


Fig. 8. Number of glaciers and area covered per size class and for each sector, the whole of Greenland and marine terminating glaciers.

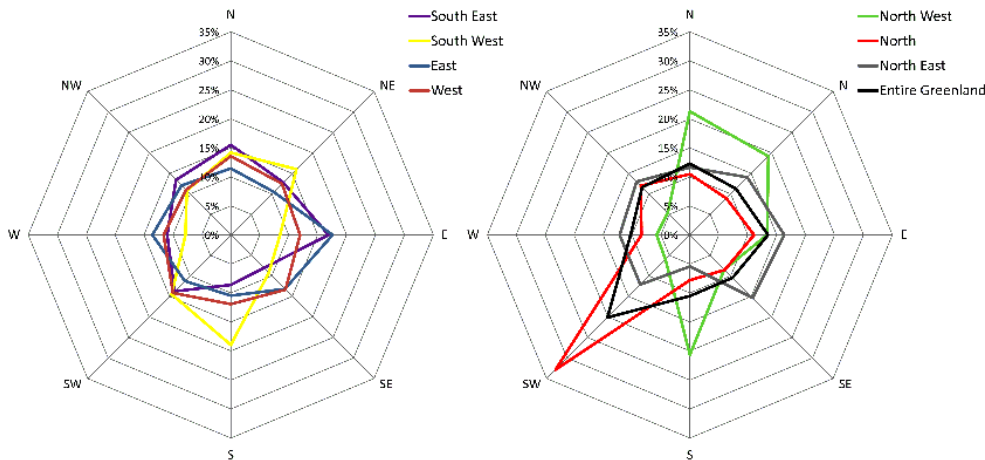
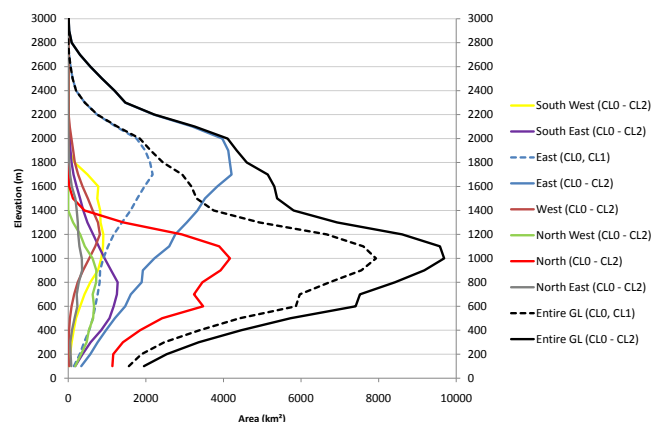


Fig. 9. Area distribution versus aspect per sector for all GIC with CL0 and CL1.

caps also creates a drop in the ice-covered area below 1000 m for all glaciers. In contrast, the other sectors contain much less ice and its distribution with elevation is more homogeneous. Maximum coverage is found around 900 and 1200 m a.s.l. The lower elevation of glacier complexes in the southern sector hints at a generally higher MAAT (or much higher

precipitation) than in the north. The CL2 glaciers increase the area covered for the eastern sector considerably, whereas in the north this is not the case as nearly all ice caps are disconnected from the ice sheet. Above 2000 m a.s.l. ice is only found in the eastern sector and the area-elevation distribution is thus the same as for Greenland as a whole. Taken together,





**Fig. 10.** Area-elevation distribution in 100 m bins for the seven sectors and all GIC. Dotted lines show the hypsometry for GIC with CL0 and CL1 only.

most of the ice ( $\sim 56\%$ ) is found between 600 and 1400 m with the peak at 1000 m a.s.l.

In Fig. 11 the spatial distribution of median elevation is shown as colour-coded circles for all GIC. A strong increase in median elevation from the coast to the interior can be seen all around Greenland with lowest values closest to the coast (0–500 m) and increasingly higher values (up to  $\sim 3000$  m) towards the interior.

## 5 Discussion

### 5.1 Assignment of connectivity levels

The assignment of connectivity levels and the rules for subdividing glacier complexes into glaciers are certainly a matter for discussion. Weidick et al. (1992) already mentioned the separation of the local GIC from the ice sheet as a major problem for Greenland, but since then no consistent solution for the whole of Greenland was presented. Assigning connectivity levels 0 and 1 (CL0 and CL1) was in most cases straight forward due to clearly identifiable drainage divides. We introduced CL2 to have strongly connected local GIC available for both, ice sheet modellers who traditionally included them in the ice sheet and GIC modellers who see them as separate entities. The hydrologic divides as derived from watershed analysis are obtained objectively, but need some editing and human interpretation to serve both communities. With the interpretation provided here we have provided a useful and sufficiently flexible solution. When better suggestions for a consistent separation come up, e.g. based on a more precise DEM or a more appropriate approach, it is possible to refine the divides in the digital database. The manual correction of the drainage divides was time consuming, but clearly faster than the manual correction of the glacier mapping errors (debris, shadow, seasonal snow). According to our rules, the Julianehåb and Ingfield ice domes have been

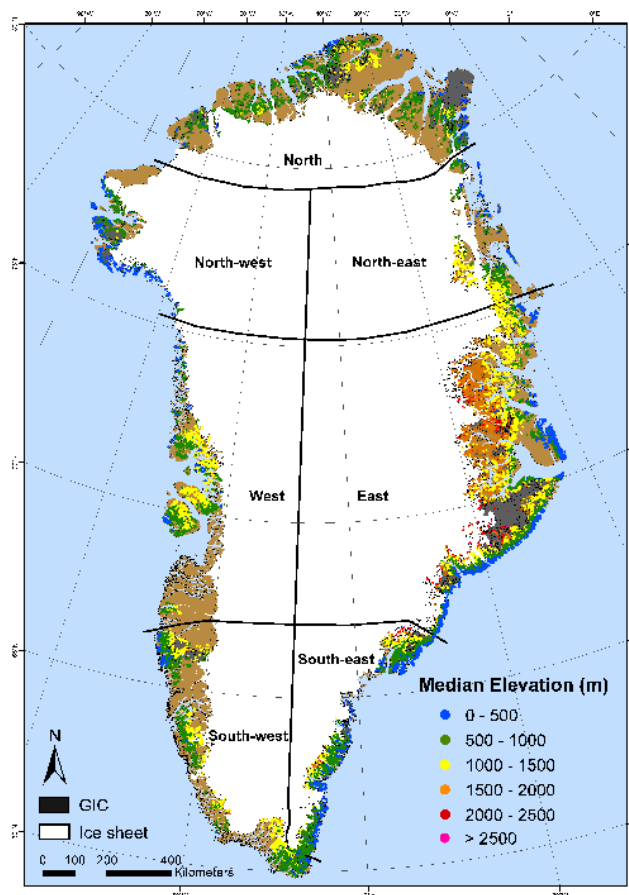


**Fig. 11.** Colour-coded visualisation of median elevation for all GIC. The mapped local GIC are shown in dark grey in the background. (min median elevation: 12 m, max median elevation: 3100 m).

interpreted as being part of the ice sheet in our inventory. Weidick et al. (1992), however, counted these ice masses as being local, but this is not compliant with the extent used in current ice sheet models (e.g. Fettweis et al., 2008). We have thus decided to exclude them completely from the local GIC.

### 5.2 Comparison to other datasets

The comparison of the total area for all glaciers  $> 0.05$  km<sup>2</sup> with CL0 connectivity to the other two available Greenland-wide datasets (DCW, GIMP) listed in Table 2 reveals that the area is highest in our dataset ( $65\,474 \pm 2029$  km<sup>2</sup>), second highest in the GIMP dataset ( $61\,610$  km<sup>2</sup>) and lowest in the DCW dataset ( $57\,715$  km<sup>2</sup>). This indicates that the generalisation in the DCW and the partly missing debris cover in the GIMP outlines make quite a difference ( $-12\%$  and  $-6\%$ , respectively) for the total area covered. The glacier outlines from the hydrologic layer of the DCW are obtained from digitized 1:1 000 000 scale topographic maps (Danko, 1992) and are thus expected not to include most of the smaller glaciers.

**Table 2.** Available vector datasets of covering the local GIC on Greenland and their differences. The “area covered (GIC)” row refers to connectivity levels CL0 and CL1. The entire dataset of this study includes the improved GIMP dataset (covering 14 068 km<sup>2</sup>) in the northernmost part of Greenland.

	DCW	GIMP	new inventory
Source	Maps 1 : 1 000 000	optical/radar	Landsat + GIMP
Period	1950s–1980s	1999–2001	1999–2004
Generalisation	high	none	none
Drainage divides	no	no	yes
Spatial resolution	approx. 2 km	15 m	30 m
Smallest unit mapped	0.1 km <sup>2</sup>	0.05 km <sup>2</sup>	0.05 km <sup>2</sup>
Debris cover included?	yes	no	yes
Northernmost region included?	yes	yes	Yes, (improved GIMP)
Availability	free	free	free
Area covered (GIC)	57 715 km <sup>2</sup>	61 610 km <sup>2</sup>	65 474 ± 2029
Area covered (total)	1 825 030 km <sup>2</sup>	1 798 960 km <sup>2</sup>	1 808 575 km <sup>2</sup>

Earlier studies used a wide range of techniques to estimate the total area covered by local GIC (cf. Sect. 1 or Cogley, 2012). The values derived here ( $\sim 89\,720 \pm 2781$  km<sup>2</sup> for CL0 and CL1,  $\sim 130\,076 \pm 4032$  km<sup>2</sup> incl. CL2) are about 50 % and 100 % larger than the mean value ( $\sim 62\,600$  km<sup>2</sup>) of the more recent previous estimates (e.g. Ohmura, 2009; Weidick and Morris, 1998; Dowdeswell and Hambrey, 2002). It has to be noted that Weidick and Morris (1998) also include CL2 GIC in their estimate as well as some larger ice domes (e.g. Julianehåb) that are not included in our assessment. The much higher total area found here implies that also the volume of the local GIC (and hence their potential sea-level rise contribution) might be higher than assumed in previous studies.

Comparing the entire ice-covered area in Greenland with the results from Kargel et al. (2012) reveals a difference of only 7480 km<sup>2</sup>, which is less than 0.5 %. Other estimates calculated this area as  $1.765 \times 10^6$  km<sup>2</sup> from the union of all pixels in a MODIS image composite that was acquired over twelve years ([http://bprc.osu.edu/wiki/Mapping\\_Land\\_Ice](http://bprc.osu.edu/wiki/Mapping_Land_Ice)) or as  $1.756 \times 10^6$  km<sup>2</sup> derived from a 1 : 2 500 000 map (Weidick and Morris, 1998).

### 5.3 Inventory data

The distribution of the area and number of glaciers with the size class is similar to distributions reported for other regions, but has locally also deviations due to the dominant presence of large ice caps. The total number of GIC (20 300) depends on the algorithm used for creating divides. The latter also determine, along with the topography in each sector, the aspect distribution presented here. Hence, using another DEM or other rules to create the divides will also result in a different number of glaciers and aspect distribution. It has also to be noted that the mean aspect of ice caps is rather arbitrary, even when they are divided into entities. The mean or median elevation did not appear to depend on aspect as in other re-

gions (Evans and Cox, 2005), but rather on the distance from the coast. Interpreting the median elevation as a proxy for the equilibrium line altitude (ELA) and hence as an indicator of the precipitation amount (e.g. Braithwaite and Raper, 2009), a decreasing precipitation trend from the coast to the interior of Greenland can be inferred. Such a trend was also found in previous studies and other regions with a maritime climate (Le Bris et al., 2011; Jiskoot et al., 2003, 2012; Paul et al., 2011; Weidick et al., 1995), and is confirmed here from an interpretation of the topographic glacier parameters for the entire perimeter of Greenland. Deriving such a trend from direct measurements is difficult, because weather stations in Greenland are either coastal (Danish Meteorological Institute stations) or located on the ice sheet (GC-Net and PROMICE Network) (Ahlstrøm et al., 2008; Steffen and Box, 2001).

### 5.4 DEM quality impacts

The quality of the DEM impacts on the inventory. As a DEM with a high spatial resolution (e.g. 30 m) and quality (e.g. no artefacts) is not available so far, we have given preference to the “low resolution with sufficient quality” version of the GIMP DEM. It had clear advantages for delineating the drainage divides in the accumulation areas compared to the higher resolution GDEM, and topographic parameters were not much different from the GDEM. The VFP DEM used for the northernmost part of Greenland was the only dataset available. It is difficult to determine the quality of this DEM, but at least the visual inspection (hillshade) revealed its general suitability. Until a higher resolution and more precise DEM is available for the entire region (e.g. from the TanDEM-X mission), the values calculated here have likely the highest quality possible today.

### 5.5 Accuracy

Apart from the methodological constraints, for example related to the position of ice divides and the interpretation of

perennial snow fields, we find that the accuracy of the glacier outlines is similar to that reported in other studies having applied automated glacier mapping in combination with manual correction (e.g. Paul et al., 2002, 2012; Bolch, 2007; Bolch et al., 2010). We derived an area uncertainty of about 3% in the mean over all glaciers with the buffer method, but this value can be much higher for individual glaciers and those with debris cover. The latter could mostly be delineated rather accurately, because solar elevation is low at the latitude of Greenland and thus provides sufficient illumination differences. However, for small glaciers and those located in regions of permafrost, the issue is more challenging. Accurate mapping of ice caps is more straightforward due to the missing debris cover, but attached snow patches (either seasonal or perennial) introduced considerable uncertainty, in particular in the northern sector of the study region.

In the same region, the impact of the missing glacier area in the SLC-off scenes from Landsat ETM+ acquired after 2002 is locally non-negligible, but overall smaller than other uncertainties. Without using these scenes it would have been nearly impossible to determine whether some of the mapped features were glaciers or not. In this regard, the mosaicking of several SLC-off scenes with much less snow cover than in the SLC-on scenes was worth the effort.

We also analysed the error due to re-projection between the UTM and the Greenland Lambert Azimuthal Equal Area projection system with latitude, and found mean area differences of 0.02% in the south and 0.05% in the north. Hence, they are two orders of magnitude smaller and negligible.

## 6 Summary

We presented the first glacier inventory for the whole of Greenland based on the classification of multispectral satellite imagery and manual editing of more than 70 Landsat scenes obtained from <http://glovis.usgs.gov/>. Additionally, we included data from an ice-cover map (<http://bprc.osu.edu/GDG/icemask.php>) for the northernmost part of Greenland that is not covered by Landsat. The new inventory revealed a 50% greater total area ( $89\,720 \pm 2781 \text{ km}^2$ ) than in the mean of the more recent previous estimates. Counting also glaciers with a strong connectivity to the ice sheet (CL2) as being local, the total area is  $130\,076 \pm 4032 \text{ km}^2$  from  $\sim 20\,300$  entities (of which about 900 are marine terminating with an area of  $64\,975 \pm 2014 \text{ km}^2$ ). The much higher area indicates the importance of assigning connectivity levels to each entity to have samples serving the needs of different user communities. While this assignment could be implemented more or less automatically, the separation of the local GIC into entities was tedious and time consuming work. Though the quality of the inventory differs regionally, the presented inventory is in our opinion the best possible dataset available to date. However, as the location of drainage divides depends on the DEM used and the rules applied for subdividing glacier

complexes, differences to other or future assessments can be expected. In any case, the differences between the datasets compared here have nothing to do with real area changes of the local GIC.

The correction of the automatically mapped glacier outlines (e.g. for debris, shadow and snow) took about 80% of the glacier mapping workload. Excluding glaciers smaller than  $0.05 \text{ km}^2$  helped to reduce the uncertainty due to seasonal snow. Applying a 1/2 pixel buffer around all outlines revealed an overall area uncertainty of 3%. The obtained size-class distributions are in general similar to those found in other regions, but are slightly different in regions dominated by ice caps. The largest number of local GIC is found in the east sector and the smallest in the west sector, largely due to the different topography of the two regions. Most of the ice is found around 1700 m a.s.l. in the East sector and around 1000 m a.s.l. in all other sectors. A dependence of glacier area on aspect was only found in the North and South sectors. The Median elevation strongly increased with the distance from the coast, indicating decreasing precipitation amounts towards the interior of Greenland. In view of current approaches to determine the future evolution of GIC under various scenarios of climate change at a global scale, we recommend using the outlines from the CL0 and CL1 GIC in combination with the GIMP DEM.

**Supplementary material related to this article is available online at: <http://www.the-cryosphere.net/6/1483/2012/tc-6-1483-2012-supplement.pdf>.**

*Acknowledgements.* This work was supported by the ESA project Glaciers\_cci (4000101778/10/I-AM) and funding from the ice2sea programme from the European Union 7th Framework Programme, grant number 226375. Ice2sea contribution number 097. H. M. acknowledges funding from the Programme for Monitoring of the Greenland Ice Sheet (PROMICE). Landsat scenes were obtained from USGS (<http://glovis.usgs.gov/>), and MODIS scenes from the NASA-Reverb website (<http://reverb.echo.nasa.gov/reverb/>). Glacier outlines in the north of Greenland were downloaded from the Ohio State University – Byrd Polar Research Center webpage (<http://bprc.osu.edu/GDG/icemask.php>). We gratefully acknowledge Paul Leclercq for his help with the digitizing of some regions in SW Greenland, Ian Howat for providing the GIMP DEM, Michael Phillip Stainsby for proof reading the paper, and H. Jiskoot and G. Cogley for the thorough reviews.

Edited by: C. O’Cofaigh

## References

- Ahlstrøm, A. P., Gravesen, P., Bech Andersen, S., van As, D., Citterio, M., Fausto, R. S., Nielsen, S., Jepsen, H. F., Kristensen, S. S., Christensen, E. L., Stenseng, L., Forsberg, R., Hanson, S., and Petersen, D.: A new programme for monitoring the mass loss of the Greenland ice sheet, *Geological Survey of Denmark and Greenland Bulletin*, 15, 61–64, 2008.
- Arendt, A., Bolch, T., J.G. Cogley, J.G. Gardner, A., Hagen, J.-O., Hock, R., Kaser, G., Pfeffer, W.T., Moholdt, G., Paul, F., Radić, V., Andreassen, L., Bajracharya, S., Beedle, M., Berthier, E., Bhambri, R., Bliss, A., Brown, I., Burgess, E., Burgess, D., Cawkwell, F., Chinn, T., Copland, L., Davies, B., De Angelis, H., Dolgova, E., Filbert, K., Forester, R., Fountain, A., Frey, H., Giffen, B., Glasser, N., Gurney, S., Hagg, W., Hall, D., Haritashya, U.K., Hartmann, G., Helm, C., Herreid, S., Howat, I., Kapustin, G., Khromova, T., Kienholz, C., Koenig, M., Kohler, J., Kriegel, D., Kutuzov, S., Lavrentiev, I., LeBris, R., Lund, J., Manley, W., Mayer, C., Miles, E., Li, X., Menounos, B., Mercer, A., Moelg, N., Mool, P., Nosenko, G., Negrete, A., Nuth, C., Pettersson, R., Racoviteanu, A., Ranzi, R., Rastner, P., Rau, F., Raup, B.H., Rich, J., Rott, H., Schneider, C., Seliverstov, Y., Sharp, M., Sigurdsson, O., Stokes, C., Wheate, R., Winsvold, S., Wolken, G., Wyatt, F., and Zheltykhina, N.: Randolph Glacier Inventory [v2.0]: A Dataset of Global Glacier Outlines. Global Land Ice Measurements from Space, Boulder Colorado, USA, Digital Media, 2012.
- Bales, R. C., Guo, Q., Shen, D., McConnell, J. R., Du, G., Burkhart, J. F., Spikes, V. B., Hanna, E., and Cappelen, J.: Annual accumulation for Greenland updated using ice core data developed during 2000–2006 and analysis of daily coastal meteorological data, *J. Geophys. Res.*, 114, D06116, doi:10.1029/2008JD011208, 2009.
- Bishop, M. P., Olsenholler, J. A., Shroder, J. F., Barry, R. G., Raup, B. H., Bush, A. B. G., Copland, L., Dwyer, J. L., Fountain, A. G., Haeberli, W., Kääh, A., Paul, F., Hall, D. K., Kargel, J. S., Molnia, B. F., Trabant, D. C., and Wessels, R.: Global Land Ice Measurements from Space (GLIMS): remote sensing and GIS investigations of the Earth's cryosphere, *Geocarto International*, 19, 57–84, 2004.
- Bolch, T.: Climate change and glacier retreat in northern Tien Shan (Kazakhstan/Kyrgyzstan) using remote sensing data, *Global Planet. Change*, 56, 1–12, 2007.
- Bolch, T., Menounos, B., and Wheate, R.: Landsat-based inventory of glaciers in western Canada, 1985–2005, *Remote Sens. Environ.*, 114, 127–137, 2010.
- Box, J. E., Bromwich, D. H., Veenhuis, B. A., Bai, L. S., Stroeve, J. C., Rogers, J. C., Steffen, K., Haran, T., and Wang, S. H.: Greenland Ice Sheet Surface Mass Balance Variability (1988–2004) from Calibrated Polar MM5 Output, *J. Climate*, 19, 2783–2800, 2006.
- Braithwaite, R. J. and Raper, S. C. B.: Estimating equilibrium-line altitude (ELA) from glacier inventory data, *Ann. Glaciol.*, 50, 127–132, 2009.
- Bull, C. and Studies, O. S. U. I. of P.: Glaciological reconnaissance of the Sukkertoppen ice cap, south-west Greenland, Ohio State University, Institute of Polar Studies, 813–816, 1963.
- Burgess, E. W., Forster, R. R., Box, J. E., Mosley-Thompson, E., Bromwich, D. H., Bales, R. C., and Smith, L. C.: A spatially calibrated model of annual accumulation rate on the Greenland Ice Sheet (1958–2007), *J. Geophys. Res.*, 115, F02004, doi:10.1029/2009JF001293, 2010.
- Cappelen, J., Laursen, E. V., Jørgensen, P. V., and Kern-Hansen, C.: DMI monthly Climate Data Collection 1768–2006, Denmark, The Faroe Islands and Greenland, Technical Report 07-06, 2007.
- Citterio, M. and Ahlstrøm, A. P.: Brief communication “The aerophotogrammetric map of Greenland ice masses”, *The Cryosphere Discuss.*, 6, 3891–3902, doi:10.5194/tcd-6-3891-2012, 2012.
- Citterio, M., Paul, F., Ahlstrom, A. P., Jepsen, H. F., and Weidick, A.: Remote sensing of glacier change in West Greenland: accounting for the occurrence of surge-type glaciers, *Ann. Glaciol.*, 50, 70–80, 2009.
- Cogley, G.: The Future of the World's Glaciers. In: *The Future of the World's Climate*, edited by: Henderson-Sellers, A. and McGuffie, K., Elsevier, Amsterdam, 197–222, 2012. 2012.
- Danko, D. M.: The digital chart of the world project, *Photogrammetric Engineering and Remote Sensing*, 58, 1125–1128, 1992.
- Dowdeswell, J. and Hambrey, M.: *Islands of the Arctic*. Cambridge: Cambridge University Press, 280 pp., 2002.
- Ettema, J., Van Den Broeke, M. R., Van Meijgaard, E., Van De Berg, W. J., Bamber, J. L., Box, J. E., and Bales, R. C.: Higher surface mass balance of the Greenland ice sheet revealed by high-resolution climate modeling, *Geophys. Res. Lett.*, 36, L12501, doi:10.1029/2009GL038110, 2009.
- Evans, I. S. and Cox, N. J.: Global variations of local asymmetry in glacier altitude: separation of northsouth and eastwest components, *J. Glaciol.*, 51, 469–482, 2005.
- Ferranti, J.: Greenland first edition DEM, available at: <http://www.viewfinderpanoramas.org/dem3.html#greenland>, 2012.
- Fettweis, X., Hanna, E., Gallée, H., Huybrechts, P., and Ericum, M.: Estimation of the Greenland ice sheet surface mass balance for the 20th and 21st centuries, *The Cryosphere*, 2, 117–129, doi:10.5194/tc-2-117-2008, 2008.
- Hammer, C. U.: *The Hans Tausen Ice Cap*, Meddelelser om Grønland, Geoscience, 39, Copenhagen, Danish Polar Center, 2001.
- Helsen, M. M., van de Wal, R. S. W., van den Broeke, M. R., van de Berg, W. J., and Oerlemans, J.: Coupling of climate models and ice sheet models by surface mass balance gradients: application to the Greenland Ice Sheet, *The Cryosphere*, 6, 255–272, doi:10.5194/tc-6-255-2012, 2012.
- Hock, R., de Woul, M., Radic, V., and Dyurgerov, M.: Mountain glaciers and ice caps around Antarctica make a large sea-level rise contribution, *Geophys. Res. Lett.*, 36, L07501, doi:10.1029/2008GL037020, 2009.
- Howat, I. and Negrete, A.: A high-resolution ice mask for the Greenland Ice Sheet and peripheral glaciers and icecaps, available at: <http://bprc.osu.edu/GDG/icemask.php> (last access: December 2012), in preparation, 2012.
- Howat, I., Negrete, A., Scambos, T., and Haran, T.: A high-resolution elevation model for the Greenland Ice Sheet from combined stereoscopic and photogrammetric data, available at: <http://bprc.osu.edu/GDG/gimpdem.php> (last access: December 2012), in preparation, 2012.
- Huss, M. and Farinotti, D.: Distributed ice thickness and volume of all glaciers around the globe, *J. Geophys. Res.*, 117, F04010, doi:10.1029/2012JF002523, 2012.
- Jiskoot, H., Murray, T., and Luckman, A.: Surge potential and drainage-basin characteristics in East Greenland, *Ann. Glaciol.*



- 36, 142–148, 2003.
- Jiskoot, H., Juhlin, D., St. Pierre, H., and Citterio, M.: Tide-water glacier fluctuations in central East Greenland coastal and fjord regions (1980s–2005), *Ann. Glaciol.*, 53, 35–44, doi:10.3189/2012AoG60A030, 2012.
- Kargel, J. S., Ahlström, A. P., Alley, R. B., Bamber, J. L., Benham, T. J., Box, J. E., Chen, C., Christoffersen, P., Citterio, M., Cogley, J. G., Jiskoot, H., Leonard, G. J., Morin, P., Scambos, T., Sheldon, T., and Willis, I.: Brief communication Greenland's shrinking ice cover: "fast times" but not that fast, *The Cryosphere*, 6, 533–537, doi:10.5194/tc-6-533-2012, 2012
- Le Bris, R., Paul, F., Frey, H., and Bolch, T.: A new satellite-derived glacier inventory for western Alaska, *Ann. Glaciol.*, 52, 135–143, 2011.
- Lemke, P.: Climate change 2007: the physical science basis: contribution of Working Group I to the Fourth Assessment Report of the Intergovernmental Panel on Climate Change, Cambridge Univ. Pr., 2007.
- Meier, M. F., Dyurgerov, M. B., Rick, U. K., O'Neel, S., Pfeffer, W. T., Anderson, R. S., Anderson, S. P., and Glazovsky, A. F.: Glaciers Dominate Eustatic Sea-Level Rise in the 21st Century, *Science*, 317, 1064–1067, doi:10.1126/science.1143906, 2007.
- Ohmura, A.: Completing the world glacier inventory, *Ann. Glaciol.*, 50, 144–148, 2009.
- Ohmura, A. and Reeh, N.: New precipitation and accumulation maps for Greenland, *J. Glaciol.*, 37, 140–148, 1991.
- Paul, F.: Melting glaciers and ice caps, *Nature Geosci.*, 4, 71–72, 2011.
- Paul, F. and Andreassen, L. M.: A new glacier inventory for the Svartisen region, Norway, from Landsat ETM+ data: challenges and change assessment, *J. Glaciol.*, 55, 607–618, 2009.
- Paul, F. and Kaab, A.: Perspectives on the production of a glacier inventory from multispectral satellite data in Arctic Canada: Cumberland Peninsula, Baffin Island, *Ann. Glaciol.*, 42, 59–66, 2005.
- Paul, F., Kaab, A., Maisch, M., Kellenberger, T. and Haerberli, W.: The new remote-sensing-derived Swiss glacier inventory: I. Methods, *Ann. Glaciol.*, 34, 355–361, 2002.
- Paul, F., Barry, R. G., Cogley, J. G., Frey, H., Haerberli, W., Ohmura, A., Ommanney, C. S. L., Raup, B., Rivera, A., and Zemp, M.: Recommendations for the compilation of glacier inventory data from digital sources, *Ann. Glaciol.*, 50, 119–126, 2009.
- Paul, F., Andreassen, L. M., and Winsvold, S. H.: A new glacier inventory for the Jostedalbreen region, Norway, from Landsat TM scenes of 2006 and changes since 1966, *Ann. Glaciol.*, 52, 153–162, 2011.
- Paul, F., Barrand, N., Berthier, E., Bolch, T., Casey, K., Frey, H., Joshi, S. P., Kononov, V., Le Bris, R., Mölg, N., Nosenko, G., Nuth, C., Pope, A., Racoviteanu, A., Rastner, P., Raup, B., Scharer, K., Steffen, S., and Winsvold, S.: On the accuracy of glacier outlines derived from remote sensing data, *Ann. Glaciol.*, 54, in press, 2012.
- Racoviteanu, A. E., Paul, F., Raup, B., Khalsa, S. J., and Armstrong, R.: Challenges and recommendations in mapping of glacier parameters from space: results of the 2008 Global Land Ice Measurements from Space (GLIMS) workshop, Boulder, Colorado, USA, *Ann. Glaciol.*, 50, 53–69, 2009.
- Radić, V. and Hock, R.: Regional and global volumes of glaciers derived from statistical upscaling of glacier inventory data, *J. Geophys. Res.*, 115, F01010, doi:10.1029/2009JF001373, 2010.
- Raper, S. C. and Braithwaite, R. J.: Low sea level rise projections from mountain glaciers and icecaps under global warming, *Nature*, 439, 311–313, 2006.
- Raup, B., Kääh, A., Kargel, J. S., Bishop, M. P., Hamilton, G., Lee, E., Paul, F., Rau, F., Soltesz, D., Khalsa, S. J. Beedle, M., and Helm, C.: Remote sensing and GIS technology in the Global Land Ice Measurements from Space (GLIMS) project, *Comput. Geosci.*, 33, 104–125, 2007.
- Rignot, E. and Mouginot, J.: Ice flow in Greenland for the International Polar Year 2008–2009, *Geophys. Res. Lett.*, 39, L11501, doi:10.1029/2012GL051634, 2012.
- Steffen, K. and Box, J. E.: Surface climatology of the Greenland ice sheet: Greenland Climate Network 1995–1999, *J. Geophys. Res.*, 106, 951–964, 2001.
- Weidick, A.: Surging glaciers in Greenland – a status, *Rapp. Grønl. Geol. Unders.*, 140, 106–110, 1988.
- Weidick, A. and Morris, E.: Local glaciers surrounding the continental ice sheets, in: *Into the Second Century of World Glacier Monitoring- Prospects and Strategies. A contribution to the IHP and the GEMS*, edited by: Haerberli, W., Hoelzle, M., and Suter, S., Prepared by the World Glacier Monitoring Service UNESCO (Chapter 12), 197–207, 1998.
- Weidick, A., Boeggild, C. E., and Knudsen, N. T.: Glacier inventory and atlas of West Greenland, *Rapp. Grønl. Geol. Unders.*, 158, 194 pp., 1992.
- Weidick, A.: Greenland, in: *Satellite image atlas of glaciers of the world*, edited by: Williams Jr., R. S. and Ferrigno, J. G., US Geological Survey Professional Paper 1386-C, 141 pp., 1995.
- Yde, J. C. and Knudsen, N. T.: Observations of debris-rich naled associated with a major glacier surge event, Disko Island, West Greenland, *Permafrost and Periglacial Processes*, 16, 319–325, doi:10.1002/ppp.533, 2005.